End-to-End Multi-Task Learning for Lung Nodule Segmentation and Diagnosis

Wei Chen (wchen@cqu.edu.cn)

Backgrounds

Backgrounds

Lung Nodule Segmentation And Diagnosis

- Lung cancer is one of the most frequently diagnosed cancers in the world, approximately 70% of which are diagnosed at advanced stages.
- An accurate segmentation mask and diagnosis result can greatly reduce the diagnostic time.
- Due to the complex visual characteristics of lung nodules, the segmentation accuracy of existing methods cannot meet the clinical needs of radiologists.
- Due to the lack of interpretable diagnosis results, radiologists are often confused about the automatic malignancy prediction results.

Backgrounds

Related Work

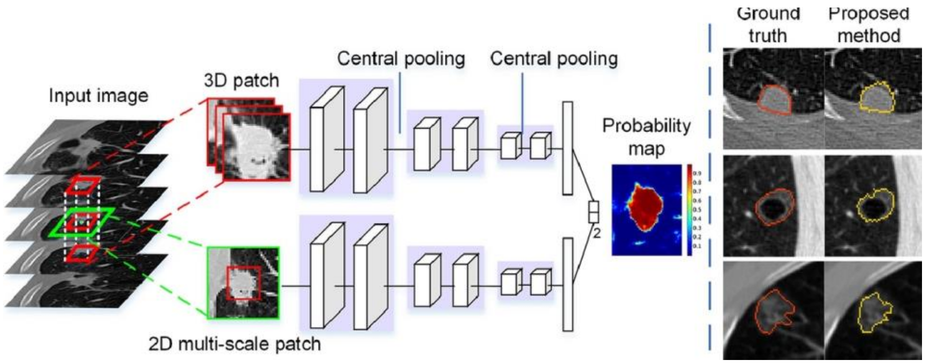

S. Wang, M. Zhou, Z. Liu, Z. Liu, D. Gu, Y. Zang, D. Dong, O. Gevaert, and J. Tian, "Central focused convolutional neural networks: Developing a data-driven model for lung nodule segmentation," Medical image analysis, vol. 40, pp. 172–183, 2017.

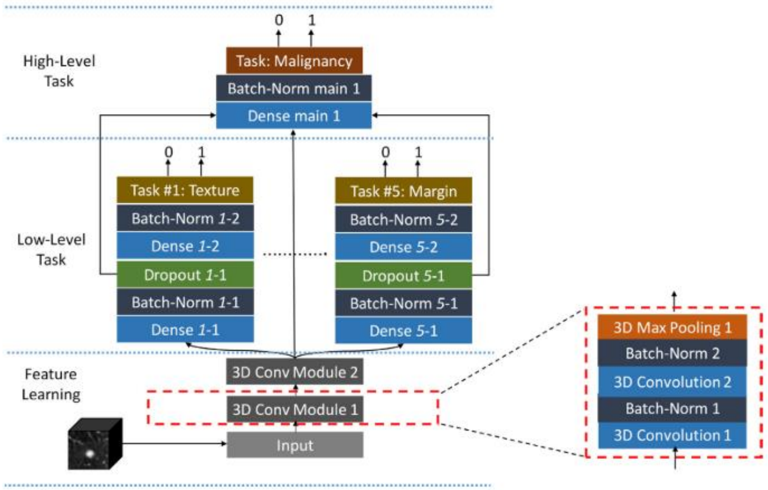

S. Shen, S. X. Han, D. R. Aberle, A. A. Bui, and W. Hsu, "An interpretable deep hierarchical semantic convolutional neural network for lung nodule malignancy classification," Expert Systems with Applications, vol. 128, pp. 84–95, 2019.

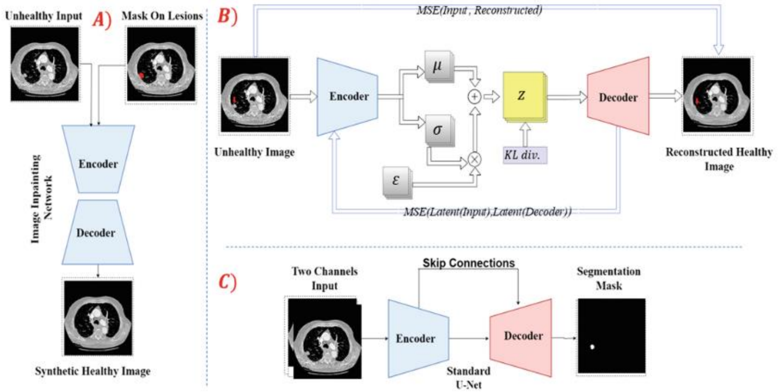

M. Astaraki, I. Toma-Dasu, O.Smedby, and C. Wang, "Normal appearance autoencoder for lung cancer detection and segmentation," in International Conference on Medical Image Computing and ComputerAssisted Intervention. Springer, 2019, pp. 249–256.

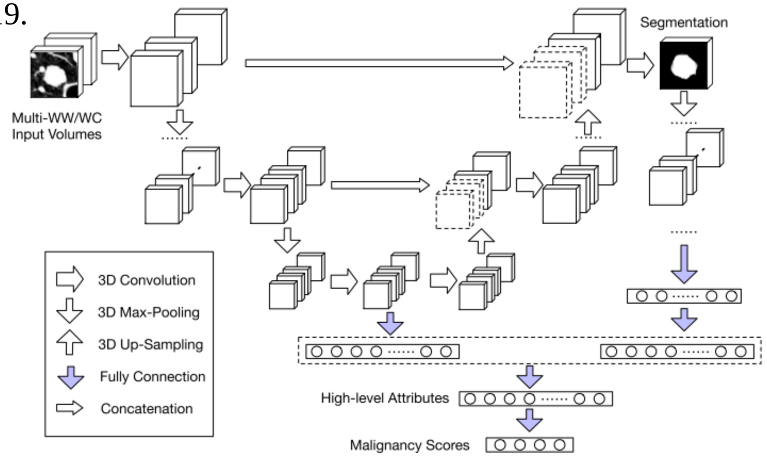

B. Wu, Z. Zhou, J. Wang, and Y. Wang, "Joint learning for pulmonary nodule segmentation, attributes and malignancy prediction," in 2018 IEEE 15th International Symposium on Biomedical Imaging (ISBI 2018). IEEE, 2018, pp. 1109–1113.

End-to-End Multi-Task Learning for Lung Nodule Segmentation and Diagnosis

End-to-End Multi-Task Learning

Architecture

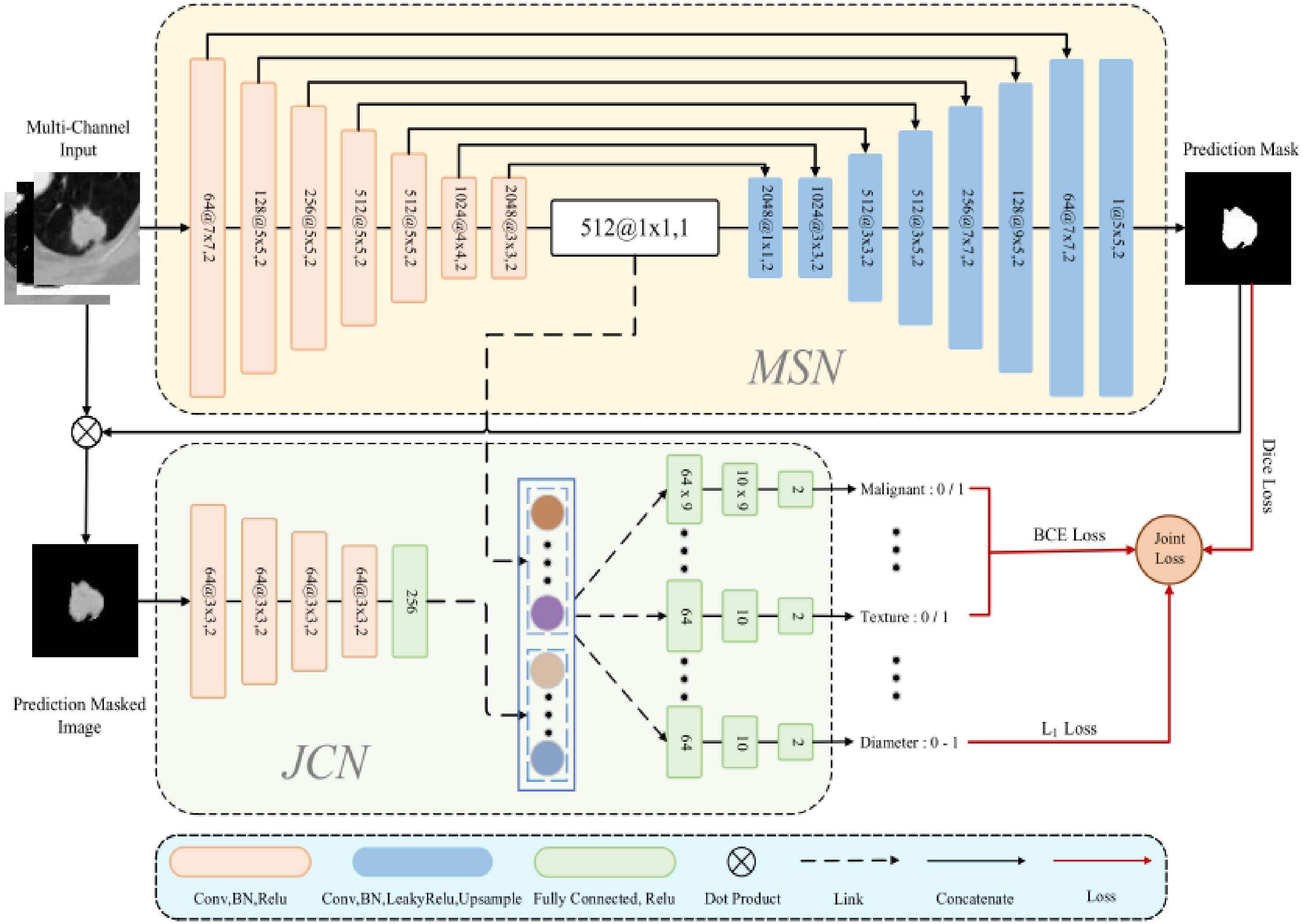

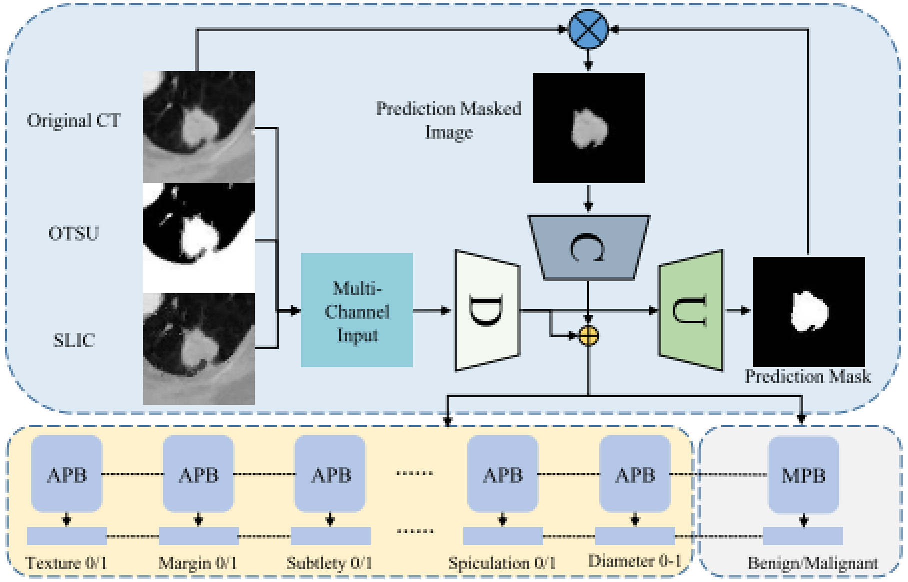

$$\mathcal{L}_{Dice} = 1 - \frac{2\sum_i^M y_p y_{gt}}{\sum_i^M y_p + \sum_i^M y_{gt}},$$

$$\mathcal{L}_{apl}^i = -(y\log(\sigma(\hat{y})) + (1-y)\log(1-\sigma(\hat{y})))$$

$$\mathcal{L}_{dia} = \|y - \sigma(\hat{y})\|_1$$

$$\mathcal{L}_{joint} = \mathcal{L}_{Dice} + \sum_{i=0}^{N} \mathcal{L}_{apl}^i + \mathcal{L}_{dia}$$

End-to-End Multi-Task Learning

Multi-Channel Input

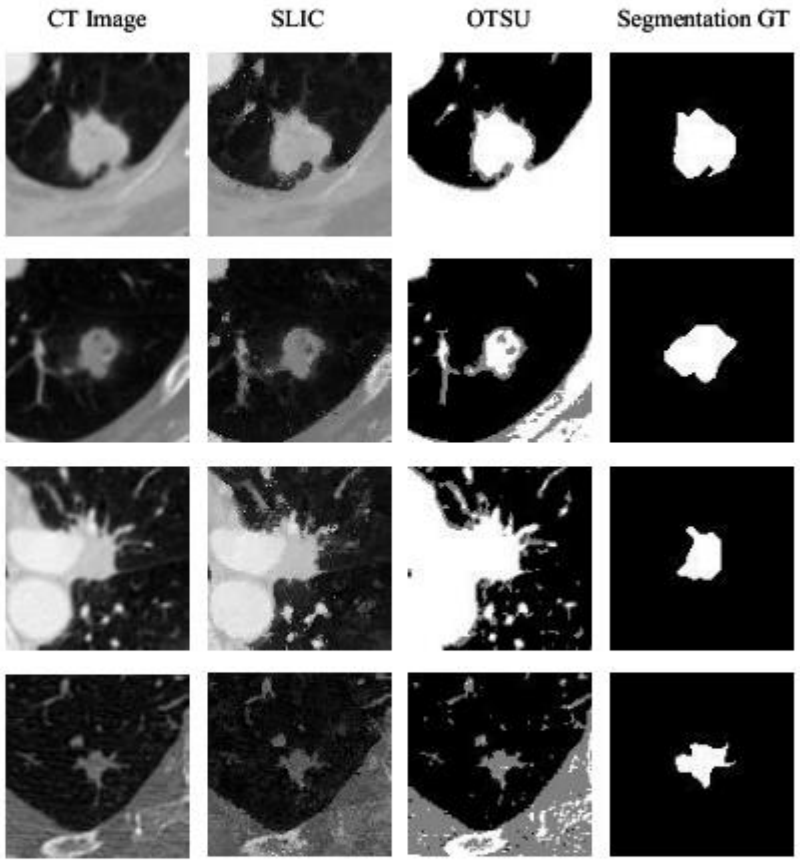

Experiments

Experiments

Lung Nodule Segmentation

TABLE II
COMPARISON BETWEEN OUR FRAMEWORK AND EXISTING METHODS ON THE LIDC–IDRI DATASET.

Method	Strategy	DSC	IoU
H. Liu et al. [34]	FCN U-Net	77.84	-
H. Liu et al. [34]	FCN V-Net	79.59	-
H. Cao et al. [22]	Dual-branch Resnet	82.74	-
Amorim et al. [21]	Multi-orientation U-Net	83.00	76.00
Tang et al. [5]	3D DCNN	83.10	71.85
Astaraki et al. [35]	2-Channels U-Net	85.86	-
Baseline	Single-Channel Single-Task	84.96	74.99
Multi-Task	Single-Channel Multi-Task	86.19	76.75
Ours	**Multi-Channel Multi-Task**	**86.43**	**77.14**

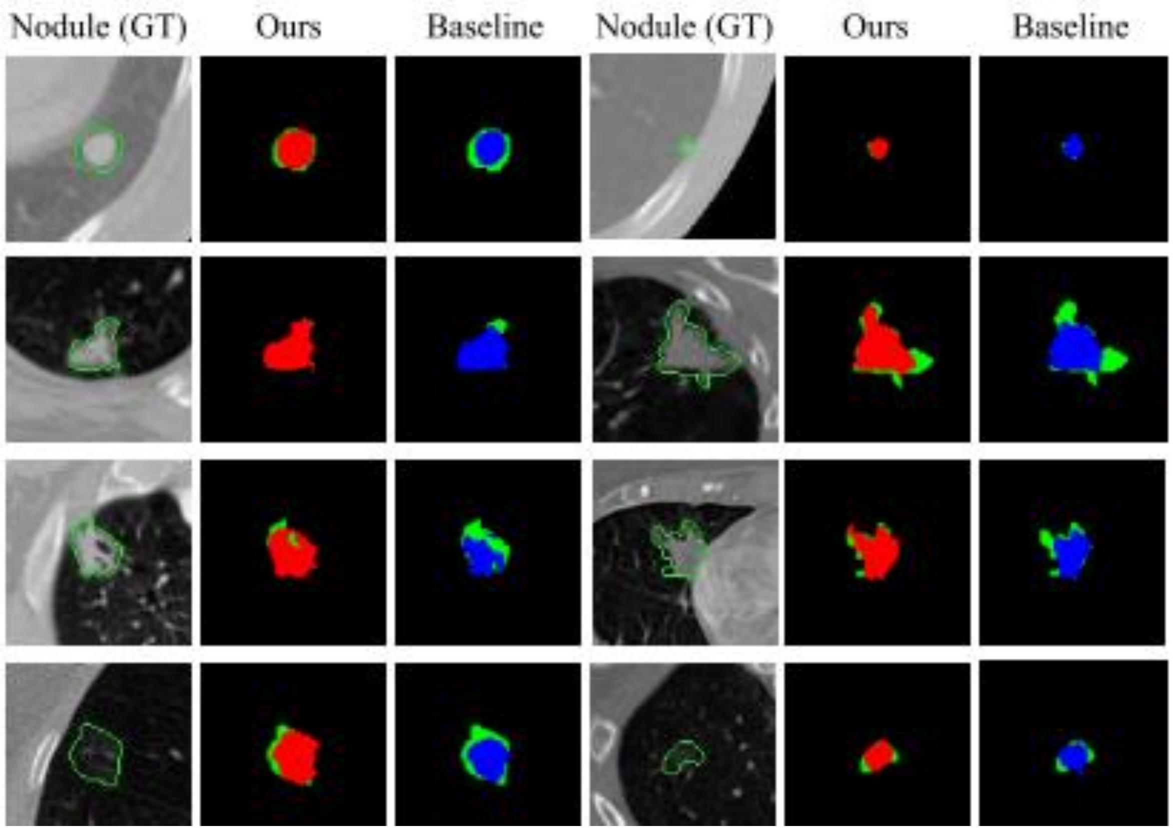

Visualized segmentation results of the proposed framework (red color) and baseline (blue color, single-channel single-task). The green color represents the ground truth.

Experiments

lung nodule diagnosis

TABLE III
MEDICAL FEATURES AND MALIGNANCY PREDICTION RESULTS.

Non-Explainable Methods	Texture	Spiculation	Lobulation	Margin	Sphericity	Calcification	Subtlety	Malignancy
3D Multi-Scale + RF [36]	-	-	-	-	-	-	-	86.84
3D Multi-Crop [37]	-	-	-	-	-	-	-	87.14
Interpretable Methods	-	-	-	-	-	-	-	-
3D Dual-Path-Dense HSCNN [4]	83.4	-	-	72.50	55.20	90.80	71.90	84.20
X-Caps [26]	**93.10**	75.23	70.69	**84.14**	**85.14**	-	**90.39**	86.39
Ours single-channel	87.32	93.57	94.38	78.52	67.70	94.07	67.51	86.33
Ours multi-channel	89.00	**93.75**	**94.75**	78.88	68.63	**94.07**	70.77	**87.07**

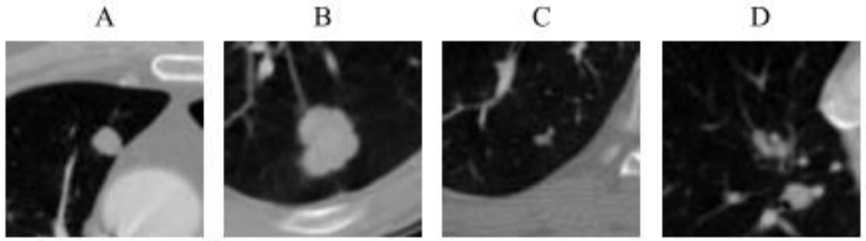

Nodu	Sub	Cal	Sph	Mar	Lobu	Spicu	Tex	Mali
A	1/1	1/1	1/1	1/1	0/0	0/0	1/1	1/1
B	1/1	1/1	1/1	1/1	1/1	0/0	1/1	1/1
C	0/0	1/1	0/0	1/1	0/1	0/0	1/1	0/0
D	0/0	1/1	1/1	0/0	0/0	0/0	1/1	0/0

THANKS